Zoosyst. Evol. 102 (2) 2026, 457–469 | DOI 10.3897/zse.102.172564

Unveiling hidden gonodactylid diversity in the South China Sea provides insights into non-monophyly of *Gonodactylellus* (Crustacea, Stomatopoda, Gonodactylidae)

Shanshan Zheng[1,2], Yanrong Wang[1], Liwen Zhang[1], Zhongli Sha[1,2,3], Jiao Cheng[1]

1 *Laboratory of Marine Organism Taxonomy and Phylogeny, Shandong Province Key Laboratory of Marine Biodiversity and Bio-resource Sustainable Utilization, Institute of Oceanology, Chinese Academy of Sciences, Qingdao, Shandong, China*

2 *University of Chinese Academy of Sciences, Beijing, China*

3 *Laboratory for Marine Biology and Biotechnology, Qingdao Marine Science and Technology Center, Qingdao, Shandong, China*

https://zoobank.org/BF3371E6-18E6-435B-B2BF-AAE79D5D13B1

Corresponding author: Jiao Cheng (jcheng@qdio.ac.cn)

Academic editor: M. Christodoulou ♦ **Received** 19 September 2025 ♦ **Accepted** 16 February 2026 ♦ **Published** 10 March 2026

Abstract

The stomatopod family Gonodactylidae Giesbrecht, 1910 comprises ecologically important predators in coral reef ecosystems, yet its phylogenetic relationships remain poorly resolved, particularly within the genus *Gonodactylellus* Manning, 1995. Despite the growing number of known species in this genus, research in the South China Sea (SCS)—a widely recognized marine biodiversity hotspot—remains limited. To address these gaps, we performed an integrative taxonomic analysis of 53 gonodactylid specimens collected from the SCS, combining detailed morphological examinations with molecular species delimitation based on the COI barcode gene. Our results revealed substantially underestimated diversity within *Gonodactylellus* in the SCS, including a new record of *Gonodactylellus caldwelli* Erdmann & Manning, 1998 in the region, and two phylogenetically distinct lineages representing new species: *Gonodactylellus xishaensis* **sp. nov.** and *Gonodactylellus* sp. We further reconstructed the phylogeny of Gonodactylidae by incorporating mitochondrial genomes (mitogenome) and nuclear genes (18S rRNA, 28S rRNA and H3), including nine newly generated and four previously published gonodactylid mitogenomes. All phylogenetic reconstructions, including those based on an extensive COI dataset with wide taxon coverage and those using a reduced taxon set with multi-gene dataset, consistently rejected the monophyly of *Gonodactylellus*, with *Gonodactylus* Berthold, 1827 nested within it, indicating a close affinity between these two genera. These findings highlight the SCS as a reservoir of previously underestimated gonodactylid diversity and underscore the persistent phylogenetic complexity of *Gonodactylellus*.

Key Words

Cryptic diversity, *Gonodactylellus*, integrative taxonomy, marine biodiversity hotspot, new species

Introduction

The order Stomatopoda (mantis shrimp) represents an extraordinary lineage of marine crustaceans that have captivated biologists through their evolutionary innovations in sensory systems and predatory adaptations. Within this group, the family Gonodactylidae is a critical component of coral reef ecosystems, where its members function as apex predators regulating tropical nutrient cycling networks (Patek and Caldwell 2005; Cronin et al. 2014). Gonodactylids exhibit remarkable morphological specializations to complex reef environments, including six rows of rectangular mid-band ommatidia enabling hyperspectral vision (Thoen et al. 2014), and raptorial appendages with smashing dactyls optimized for high-velocity strikes (Patek et al. 2004). Despite their ecological and evolutionary significance, systematic understanding of Gonodactylidae remains fragmented (Barber and Boyce

Copyright *Zheng, S. et al.* This is an open access article distributed under the terms of the Creative Commons Attribution License (CC BY 4.0), which permits unrestricted use, distribution, and reproduction in any medium, provided the original author and source are credited.

2006; Van Der Wal et al. 2017, 2025; Palecanda et al. 2020), which is particularly true for the most species-rich gonodactylid genus, *Gonodactylellus* Manning, 1995.

Gonodactylellus was originally separated from *Gonodactylus* Berthold, 1827 based on morphological characteristics, including a significantly smaller body size (total length < 55 mm) and narrow ocular scales (Manning 1978). Concurrently, the genus *Gonodactylus* was strictly restricted to five large-sized species (e.g., *Gonodactylus chiragra* Fabricius, 1781, *Gonodactylus smithii* Pocock, 1893), thereby excluding several previously classified small to medium-sized species (Manning 1995). This morphology-based classification, however, has been challenged by molecular phylogenetic evidence. Barber and Erdmann (2000), based on mitochondrial cytochrome oxidase subunit I (COI) sequence analyses, revealed significant polyphyly within *Gonodactylellus*, where four species nested within a clade containing *Gonodactylus* and *Gonodactylinus* Manning, 1995. This result not only contradicts the morphological diagnosis of *Gonodactylellus* but also suggests that body size variation, a key diagnostic characteristic, may reflect ecological niche partitioning rather than phylogenetic divergence (Barber and Erdmann 2000). The observed non-monophyly of *Gonodactylellus*, along with unresolved relationships among *Gonodactylus* and related genera, may also suggest that there are more genus-level clades than currently recognized. Furthermore, Ahyong (2001) synonymized *Gonodactylinus* under *Gonodactylellus* based on congruent morphological characters (e.g., telson structure and ocular scale width), arguing that the former lacked any morphological distinctions justifying generic recognition. Collectively, these findings underscore that the phylogenetic relationships within gonodactylids remain substantially unresolved, particularly concerning the non-monophyly of *Gonodactylellus* and its ambiguous boundaries with *Gonodactylus*.

The South China Sea (SCS), a globally significant marine biodiversity hotspot, hosts exceptionally diverse ecosystems, such as coral reefs, mangroves, and seagrass meadows (Vo et al. 2013), that are under threat from global warming and anthropogenic pressures (Yu 2012). Despite its ecological prominence, stomatopod diversity in the SCS remains poorly documented. For instance, only 10 species of Gonodactylidae have been recorded from coral reef systems in Nansha Islands, SCS (Liu 1975, 1978; Liu and Wang 1998; Liu 2008), a sharp contrast to known diversity of this family in the tropical Indo-West Pacific (> 40 species, Global Biodiversity Information Facility, https://www.gbif.org/). This discrepancy is particularly pronounced in the genus *Gonodactylellus*, which exhibits exceptional species diversity but remains severely understudied in the SCS. The sampling challenges for *Gonodactylellus* species are compounded by their small body size and cryptic reef-dwelling behaviors, which further complicate detection and collection. Although gonodactylid mantis shrimps have been documented from several areas adjacent to the central SCS (e.g., Vietnam, Manning 1995; northern Indonesia, Ahyong and Moosa 2004; Ahyong and Erdmann 2007; and Singapore, Ahyong 2016), DNA barcoding surveys of this family have thus far been limited to Hong Kong coastal waters (Tang et al. 2010), leaving most of the regions in the SCS genetically unexplored. Therefore, conducting systematic surveys of *Gonodactylellus* diversity across the SCS within a phylogenetic framework is imperative.

Given the knowledge gaps mentioned above, we hypothesize that (i) the SCS harbors undocumented diversity within *Gonodactylellus* due to insufficient sampling and complicated morphological diagnosis of this genus, and (ii) currently, taxonomic systems of *Gonodactylus* and *Gonodactylellus* do not reflect the truly phylogenetic relationships. To address these hypotheses, we integrate detailed morphological examinations with molecular species delimitation on newlycollected stomatopod specimens from the SCS reefs supplemented by a review of historical records. Our study aims to (i) assess species diversity of Gonodactylidae in the SCS using concordant morphological and molecular evidence, with emphasis on identifying cryptic lineages, and (ii) re-evaluate the generic classification of *Gonodactylellus* by reconstructing a phylogeny using a multi-gene dataset. By providing an updated assessment of gonodactylid diversity, this work underscores the significance of the SCS as a hotspot for stomatopod biodiversity, while contributing to the foundational knowledge critical for future conservation planning.

Methods

Specimen collection and identification

A total of 53 stomatopod specimens representing three gonodactylid genera were examined in this study. These specimens were collected via SCUBA diving across reef slopes and lagoons in the SCS. Specimens were collected from coral rubble by carefully fracturing reef substrates and individually catalogued. Among them, a subset of intact individuals was photographed *in situ* to document live coloration (Suppl. material 1). All samples were fixed in 85% ethanol and deposited in the Marine Biodiversity Museum of Chinese Academy of Sciences (MBMCAS), Qingdao, China. Specimens of five additional gonodactylid species: *Gonodactylaceus ternatensis* (de Man, 1902), *Gonodactylellus affinis* (de Man, 1902), *Gonodactylellus viridis* (Serène, 1954), *Gonodactylus platysoma* Wood-Mason, 1895 and *Gonodactylus smithii* Pocock, 1893, for phylogenetic analyses were obtained from MBMCAS. The detailed sampling information is listed in Suppl. material 2: table S1.

Species identification followed the diagnostic morphological criteria established in recent taxonomic revisions (Ahyong 2001, 2012a). Morphological observations focused on key sclerotized structures: (1) cephalothoracic

morphology, including rostral plate configuration; (2) lateral processes of thoracic segments 5–8; and (3) telson and uropod armature. Specimens were grouped into morphotypes based on these characters. Morphological terminology adheres to Ahyong (2001, 2012a).

DNA extraction and sequencing

Total genomic DNA was extracted from approximately 20 mg of abdominal muscle tissue using the Omega EZNA Tissue DNA Kit (Omega Bio-Tek, Norcross, GA, USA) following the manufacturer's protocol. The quality of DNA was checked using 1% agarose gel electrophoresis and further confirmed by NanoDrop 2000 spectrophotometer.

The partial sequences of mitochondrial COI were amplified by polymerase chain reaction (PCR) using the universal primers: jgLCO1490/jgHCO2198 (Geller et al. 2013) and StoCOIF/StoCOIR (Feller et al. 2013). The PCR reaction mixture (25 µL) contained: 12.5 µL 2× Taq Master Mix (1.5 mM $MgCl_2$, Takara Bio, Japan), 1 µM each forward/reverse primer, 1 µL template DNA (20–50 ng/µL), and nuclease-free water to volume. The PCR cycling conditions included an initial denaturation at 94 °C for 3 min, followed by 35 cycles of 94 °C for 30 s, 55 °C/50 °C for 30 s depending on primer pairs and specimens, 72 °C for 1 min, and a final extension at 72 °C for 5 min. The PCR products were verified by 1% agarose gel electrophoresis and purified using the QIA-quick gel purification kit (Qiagen, Hilden, Germany). The purified PCR products were sequenced bidirectionally using the same primer pairs for PCR amplification by ABI 3730xl sequencer (Applied Biosystems, Foster City, CA, USA) with ≥ 90% forward/reverse coverage.

Raw sequencing chromatograms were processed using the SeqMan program (DNASTAR, Madison, WI, United States) for quality control with a Phred score threshold of 30 or higher, followed by primer removal and bidirectional assembly to obtain sequences. A total of 53 nucleotide sequences from 53 gonodactylid specimens were newly generated in this study (Suppl. material 2: table S1), while 69 nucleotide sequences from 33 taxa of the superfamily Gonodactyloidea (Gonodactylidae and Odontodactylidae) were obtained from GenBank as detailed in Suppl. material 2: table S2. Multiple sequence alignment was performed using the MUSCLE algorithm integrated into MEGA 12.0.8 (Kumar et al. 2016) with parameters set to 100 iterations and a gap penalty of -400. The aligned sequences were further refined using trimAl v1.5.0 (Capella-Gutiérrez et al. 2009) in automated mode to remove low-confidence regions defined by alignment consistency scores below 0.8 or gap proportions exceeding 50%. This process yielded a final trimmed alignment of 550 base pairs (bp) for COI.

For mitochondrial genome (mitogenome) sequencing, the DNA of gonodactylid species collected in this study (Suppl. material 2: table S3) was used to generate sequencing libraries using TruSeq Nano DNA HT Sample preparation Kit (Illumina, USA) following manufacturer's protocols. These libraries, containing paired-end reads with an insert size of 350 bp, were then sequenced on the Illumina NovaSeq platform. The raw reads were filtered to exclude those with an average quality value below Q20. Mitogenomes were assembled from filtered reads using Geneious Prime v2024.0.5 (Kearse et al. 2012) with a mitochondrial COI sequence from Gonodactylus platysoma (Barber and Erdmann 2000) as the seed, followed by annotation within the same software. We extracted 13 protein-coding genes (PCGs), 16S rRNA, 12S rRNA, 18S rRNA, 28S rRNA, and histone H3 (H3). Due to overlapping regions (specifically between ATP8-ATP6, ATP6-COX3, and ND4-ND4L) and four genes encoded on the complementary strand (ND1, ND4, ND4L, and ND5), overlapping nucleotide segments were duplicated to ensure complete representation of each PCG. Each gene was aligned with MUSCLE (Kumar et al. 2016), trimmed with trimAl v1.5.0 (Capella-Gutiérrez et al. 2009), and concatenated using PhyloSuite v1.2.3 (Xiang et al. 2023), resulting in a final alignment of 17,024 bp.

Species delimitation

Three commonly used species delimitation methods were used to explore the potential existence of cryptic species based on the barcoding COI dataset: Automated Species Assignment and Partitioning (ASAP), Automatic Barcode Gap Discovery (ABGD), and Bayesian Poisson Tree Processes (bPTP). Based on the COI dataset, genetic distances were calculated using the Kimura two-parameter model in MEGA to estimate both interspecific and intraspecific genetic distances (Suppl. material 2: table S4). ASAP was conducted on the online platform (https://bioinfo.mnhn.fr/abi/public/asap/) using an automated species delimitation algorithm based on genetic distance distributions. In parameter settings, the Poisson distribution model was selected to fit the genetic distance distribution, support values were calculated through 1000 bootstrap resamplings, and the probability threshold was strictly set to 0.01. ABGD analysis was performed using the ABGDpy 0.1 software package (https://github.com/iTaxoTools/ABGDpy.git) to execute distance-based automated species delimitation. The prior distance range was set to pmin = 0.001 and pmax = 0.1 with a step size of dx = 0.1 to cover taxonomic groups with different evolutionary rates. The bPTP analysis was conducted using the PTP-pyqt 5 0.1 software (https://github.com/iTaxoTools/PTP-pyqt5.git) to implement Bayesian inference-based species delimitation. A posterior probability (PP ≥ 0.95) was applied to determine whether branches represented species boundaries, ensuring statistical reliability.

Phylogenetic analyses

Phylogenetic reconstruction was performed using maximum likelihood (ML) and Bayesian inference (BI) algorithms. For the combined multi-gene dataset (Suppl. material 2: table S3), the best partitioning strategy and best-fitting substitution models for each partition were selected in ModelFinder (Kalyaanamoorthy et al. 2017). The ML analysis was conducted using IQ-TREE 2.4.0 (Trifinopoulos et al. 2016) with the optimal partition scheme and substitution model (Suppl. material 2: table S5). Branch support was assessed through 100,000 ultrafast bootstrap replicates, and bootstrap (bs) values > 60% are presented on the resulting phylogeny. The BI analysis was performed using MrBayes 3.2.7a (Ronquist et al. 2012) under the best-fitting partition scheme and model chosen based on a Bayes Factor greater than 10 (Suppl. material 2: table S5). Two independent Markov Chain Monte Carlo analyses ran simultaneously for 10 million generations with sampling every 1000 generations, and the first 25% of iterations were discarded as burn-in. After discarding burn-in trees sampled before stationarity, a 50% majority rule consensus tree was constructed from the remaining sampled trees to estimate Bayesian posterior probabilities (Pp) for each node and parameter estimates for both independent runs. Convergence and effective sample sizes exceeding 200 were verified using Tracer v1.7.2 (Rambaut et al. 2018). Pp values > 0.6 are presented on the BI topology. The resulting trees were visualized and annotated using the iTOL platform (https://itol.embl.de/).

Results

Phylogenetic analyses

The ML and BI trees constructed from 122 mitochondrial COI sequences exhibited largely congruent topologies (Fig. 1, Suppl. material 3). The results demonstrated that the genus *Gonodactylellus* is non-monophyletic, with species of *Gonodactylus* nested within it. All species from these two genera clustered together, further subdivided into two subclades. Clade I consisted exclusively of *Gonodactylellus snidsvongi* (Naiyanetr, 1987) and *Gonodactylellus barberi* Ahyong & Erdmann, 2007 with full support (100 bs, 1.00 Pp), while Clade II encompassed all remaining *Gonodactylellus* species, notably including all species of *Gonodactylus* analyzed in this study.

To overcome the limitations of COI in resolving higher-level taxonomic relationships, we further conducted phylogenetic analyses using a multi-gene dataset, incorporating mitogenomic and nuclear (18S rRNA, 28S rRNA and H3) genes. To achieve this, we newly generated mitogenomic and nuclear sequences from six species of *Gonodactylellus*, two species of *Gonodactylus*, and one species of *Gonodactylaceus*, thereby expanding the available molecular resources for the family Gonodactylidae (Suppl. material 2: table S3). With the genus *Odontodactylus* designated as the outgroup, both BI and ML analyses yielded largely congruent topologies (Fig. 2). These analyses revealed that species of *Gonodactylellus* and *Gonodactylus* formed a strongly supported clade (100 bs, 1.00 Pp), within which *Gonodactylellus* was recovered as paraphyletic. Specifically, *Gonodactylus* species formed a distinct subclade that was nested within the assemblage of *Gonodactylellus* lineages, indicating a close affinity between these two genera. This *Gonodactylellus-Gonodactylus* clade was recovered as sister to representatives of the genus *Neogonodactylus* Manning, 1995, whereas members of the genus *Gonodactylaceus* represented an earlier-diverging lineage, despite low statistical support for these deeper relationships in the ML analysis.

Species identification and delimitation

This study identified seven morphospecies based on morphological examination of 53 stomatopod specimens. Four species matched known taxa: *Gonodactylellus caldwelli* Erdmann & Manning, 1998, *Gonodactylellus espinosus* (Borradaile, 1898), *Gonodactylellus erdmanni* Ahyong, 2001, and *Gonodactylus smithii* Pocock, 1893. Notably, *G. caldwelli* represents its first recorded occurrence in the SCS. Of the remaining three morphospecies, one was identified as *Gonodactylaceus* sp. The genus *Gonodactylaceus*, diagnostically characterized by a uropodal protopod bearing one or two proximal lobes between the terminal spines, is morphologically distinct from the focal genera of this study, *Gonodactylellus* and *Gonodactylus*. Accordingly, this specimen is excluded from further discussion herein. In contrast, two others, though belonging to the genus *Gonodactylellus*, could not be assigned to any described species based on morphological characteristics and were tentatively designated as Morphogroup A and Morphogroup B.

A total of 122 mitochondrial COI gene sequences were used for the following species delimitation analysis. The three methods (ABGD, ASAP, and bPTP) yielded divergent results: ABGD identified 44 Molecular Operational Taxonomic Units (MOTUs), ASAP delineated 27 MOTUs, and bPTP supported 34 MOTUs (Fig. 1). All methods consistently recognized Morphogroups A and B as distinct species, with their phylogenetic positions significantly divergent from known gonodactylids in both ML and BI trees (100 bs, 1.00 Pp, Fig. 1, Suppl. material 3). Integrating morphological and molecular evidence, we propose: 1) Morphogroup A (represented by a single severely damaged specimen) be provisionally designated as *Gonodactylellus* sp.; 2) Morphogroup B (collected from the Xisha Islands, SCS) be formally described as *Gonodactylellus xishaensis* sp. nov. Additionally, *G. smithii*, despite its well-defined diagnostic characters, was split into two MOTUs across all analyses, possibly suggesting the presence of cryptic diversity

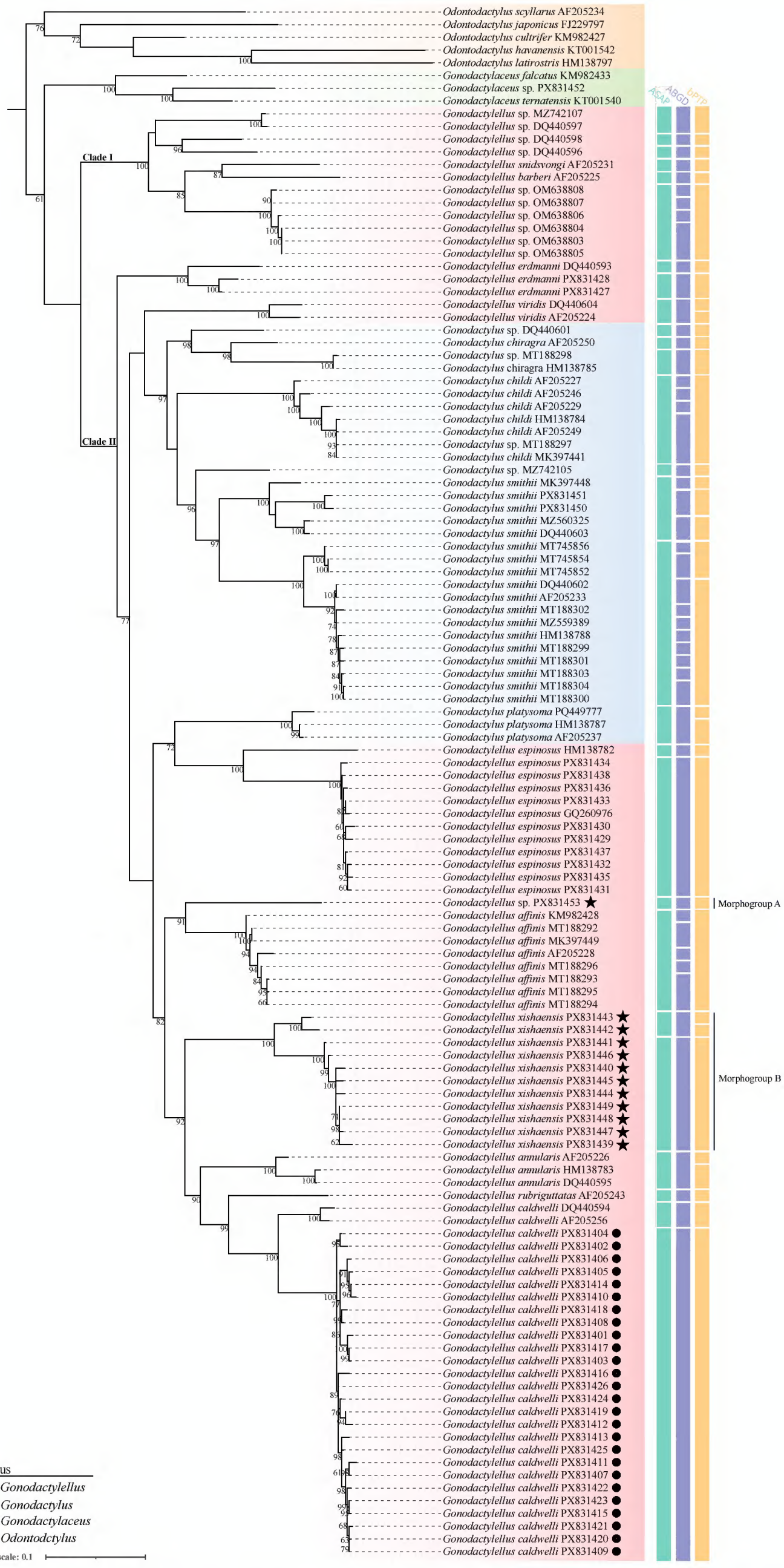

Figure 1. Maximum likelihood phylogeny reconstructed from mitochondrial COI sequences, depicting species boundaries inferred by three delimitation methods: ASAP (green), ABGD (purple), and bPTP (yellow). Symbols denote taxonomic novelties: black stars highlight proposed new species (*Gonodactylellus xishaensis* sp. nov. and *Gonodactylellus* sp.), black circles mark newly recorded species (*Gonodactylellus caldwelli*) in the SCS. Bootstrap support (bs) values > 60% are shown for key nodes.

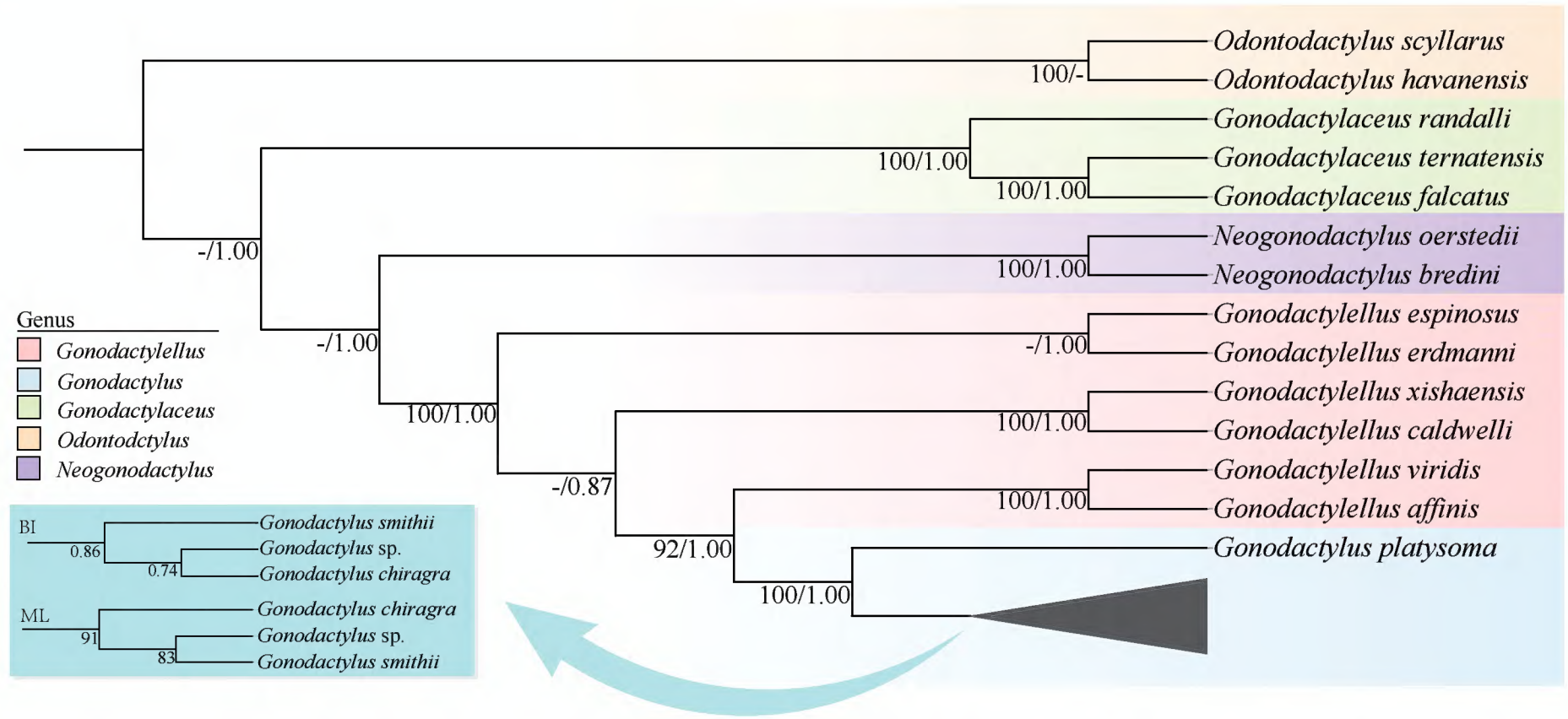

Figure 2. Maximum likelihood phylogeny based on the concatenated mitogenomic and nuclear (18S rRNA, 28S rRNA and H3) genes. Nodal support values represent maximum likelihood bootstrap (bs)/Bayesian posterior probabilities (Pp). Only bs/Pp values > 60% / 0.6 are shown.

within this taxon. Given the limited sample size and insufficient morphological or molecular evidence, we do not pursue a detailed discussion here; however, the observed genetic divergence warrants further investigation with expanded sampling.

Taxonomy, descriptions of new species and newly recorded species

Gonodactylellus xishaensis sp. nov.

https://zoobank.org/D6B53201-F825-44C0-9369-E66660593FF1

Fig. 3

Material examined. ***Holotype.*** South China Sea • female, TL 23 mm; Ximen Reef, Xisha Islands; 9°55'N, 114°26'E; depth 35 m; 23 May 2024; Ziming Yuan coll.; MBM288196.

Paratypes. South China Sea • 1 female, TL 18 mm; Robert Island, Xisha Islands; 16°30'N, 111°33'E; depth 15 m; 7 Jul. 2024; Dong Dong coll.; MBM288174 • 4 females, TL 17–23 mm; Antelope Reef, Xisha Islands; 16°28'N, 111°33'E; depth 5–9 m; 22 Aug. 2024; Dong Dong coll.; MBM288186 • 2 females, TL 17–20 mm; Quanfu Reef, Xisha Islands; 16°34'N, 111°40'E; depth 21 m; 8 Jun. 2024; Lin He coll.; MBM288191 • 1 male, 1 female, TL 23–25 mm; Ximen Reef, Xisha Islands; 9°55'N, 114°26'E; depth 35 m; 23 May 2024; Ziming Yuan coll.; MBM288196 • 1 female, TL 24 mm; Zhaoshu Dao, Xisha Islands; 16°59'N, 112°16'E; depth 20 m; 1 Jul. 2024; Dong Dong coll.; MBM288213.

Diagnosis. Ocular scales separate, rounded. Rostral plate basal portion anterolateral angles rounded; lateral margins divergent anteriorly. Raptorial claw dactylus without proximal notch in adults. Thoracic somite 6 lateral processes subequal to or slightly broader than that of thoracic somite 7. Pleopod 1 endopod with indistinct lateral lobe on endite; lateral lobe small, irregular, posterior margin with a deep notch. Telson with spiniform submedian denticles; intermediate teeth distinct, apices not reaching to apices of intermediate denticles. Abdominal somite 6 with armed intermediate and lateral bosses, submedian carinae unarmed. Telson mid-dorsal carinae swelled with posterior spine, otherwise smooth; submedian teeth spindly, intermediate teeth blunt, lateral teeth indicated by a shallow notch. Accessory median carinae short, smooth, fused with median carinae anterior, not more than half of median carina. Uropodal exopod proximal segment with setose inner margin; distal margin with spine. Uropodal endopod and distal segment of exopod with entire margin setose.

Description. Eyes elongate; cornea subconical. Ocular scales low, separate, rounded. A1 peduncle length 0.7 length of CL. A2 scale length 0.3–0.4 CL.

Rostral plate broader than long; basal portion with transverse; anterolateral angles blunt; lateral margins divergent anteriorly; median spine longer than base, laterally flattened.

Raptorial claw dactylus proximally smooth; propodus with proximal movable spine, opposable margin sparsely pectinate proximally.

Mandibular palp 2-segmented.

TS6–7 lateral processes subequal to or slightly broader than that of TS7; lower margins truncate. TS8 anterolateral margin rounded; sternal keel obsolete.

PLP1 endopod with indistinct lateral lobe on endite; lateral lobe small, irregular, with a deep notch in the posterior.

AS1–5 posterolateral angles unarmed. AS6 with armed intermediate and lateral bosses, submedian carinae unarmed; lateral boss posterolateral short, blunt.

Telson broader than long; intermediate teeth distinct, blunt, apices not reaching to apices of intermediate

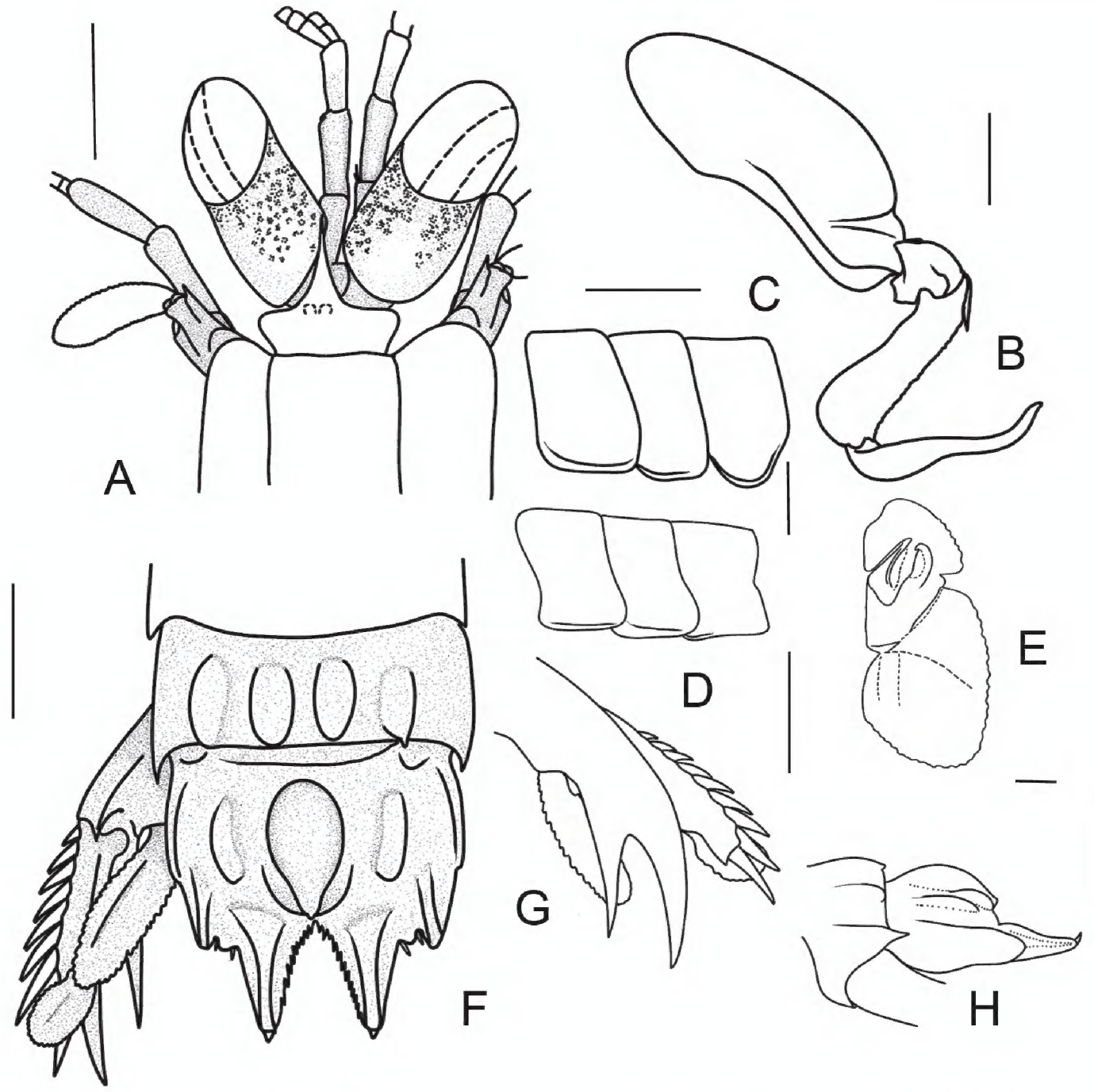

Figure 3. *Gonodactylellus xishaensis* sp. nov. female holotype (MBM288196). Morphological details. **A.** Anterior cephalon, dorsal view; **B.** Raptorial claw, right lateral view; **C.** TS6–8, left lateral view; **D.** AS3–5, left lateral view; **F.** AS5–6, telson and uropod, dorsal view; **G.** Uropod, left ventral view; **H.** Telson, left lateral view. Male paratype (MBM288196) **E.** PLP1 endopod, right anterior. Scale bars: 1 mm (**A–D, F–H**); 2 mm (**E**).

denticles; lateral teeth distinct, apex blunt, distinct well-off margin of telson. Telson median carina tumid in both sexes, accessory median carinae short, smooth, fused with median carina posteriorly, not more than half of median carina; anterior submedian carina, submedian expansion not longer than half of median carina. Telson ventral surface lacking intermediate teeth or carina on submedian.

Uropodal protopod lateral terminal spines longer; upper proximal surface with blunt spine posteriorly. Uropodal exopod proximal segment outer margin with 8–10 (usually 9) movable spines, distalmost one not exceeding apex of distal segment; inner margin setose; distal margin without ventral spine; exopod distal segment with entire margin setose. Uropodal endopod narrow, length 2.4–3.2 times the breadth; entire margin setose.

Coloration. Entire body purplish-red with unevenly distributed pale yellow spots. Swollen portion of median carina of telson orange-red, featuring a light-yellow round spot at its center. Meral spot of raptorial claw exhibiting no distinct difference from body color, being consistent with purplish-red background. After alcohol preservation, overall coloration faded, with orange-red hue of median carina of telson remaining.

Etymology. The new species is named after its type locality, Xisha Islands.

Distribution. Presently known only from the South China Sea.

Ecology. Living within the cavities of coral reefs.

Remarks. *Gonodactylellus xishaensis* sp. nov. adds to the recently described gonodactylids from the SCS, following *Gonodactylopsis maqqaba* Ahyong, 2022 from Macclesfield Bank (Ahyong 2022), suggesting that this region may harbor a higher species diversity of stomatopods than previously recognized. *G. xishaensis* sp. nov. is morphologically similar to *Gonodactylellus kume* Ahyong, 2012, *Gonodactylellus rubriguttatus* Erdmann & Manning, 1998 and *Gonodactylellus micronesicus* Manning, 1971 for having the combination of following characters: having tumid median carina on the telson, the short accessory median carinae not extending one-third of the median carina anteriorly and fused with median carina posteriorly, and the telson lacking dorsal ornamentation, such as spines, on dorsal surface (Manning 1971; Erdmann and Manning 1998; Ahyong 2001, 2012b). The new species can be distinguished from above three species by the intermediate denticles of the telson, which do not extend

beyond the posterior margin of the intermediate teeth, and the intermediate carina of the telson, which is short and reaches anteriorly at most to the posterior end of the lateral carina (Ahyong 2001, 2012b). Additionally, the new species differs from *G. kume* by the endopod of pleopod 1. In *G. xishaensis* sp. nov., the lateral lobe on the anterior endite is indistinct, small, and irregular, with a deep notch on its posterior margin; in *G. kume*, the lateral lobe on the posterior endite is not only indistinct but also narrow and small, with its margin blending continuously with (or hardly breaking from) the general outline of the distal endite (Ahyong 2012b). *G. xishaensis* sp. nov. further differs from *G. rubriguttatus* by the AS6. In *G. rubriguttatus*, the AS6 bears a distinct marginal carina and the posterolateral teeth are incurved (Erdmann and Manning 1998); in *G. xishaensis* sp. nov., the marginal carina is absent and the posterolateral teeth are acutely posteriorly directed. Relative to *G. micronesicus*, *G. xishaensis* sp. nov. has more elevated median carina on the telson (Manning 1971; Ahyong 2002).

***Gonodactylellus* sp.**

Fig. 4

Material examined. South China Sea • 1 female; North Island, Xisha Islands; 16°34'N, 111°40'E; cavities in coral reef; depth 15 m; 29 Aug. 2024; Dong Dong coll.; MBM288170.

Description. Eyes elongate; cornea subconical. Ocular scales low, separate, bases transverse. A1 peduncle length 0.6 CL.

Rostral plate broader than long; basal portion sloping posteriorly; anterolateral angles blunt; lateral margins divergent anteriorly; median spine longer than base, laterally flattened.

Raptorial claw dactylus proximal with notch; propodus with proximal movable spine, opposable margin sparsely pectinate proximally.

Mandibular palp 2-segmented.

TS6 lateral processes broader than TS7; TS6 margins truncate, TS7 and TS8 anterolateral margins rounded; sternal keel obsolete.

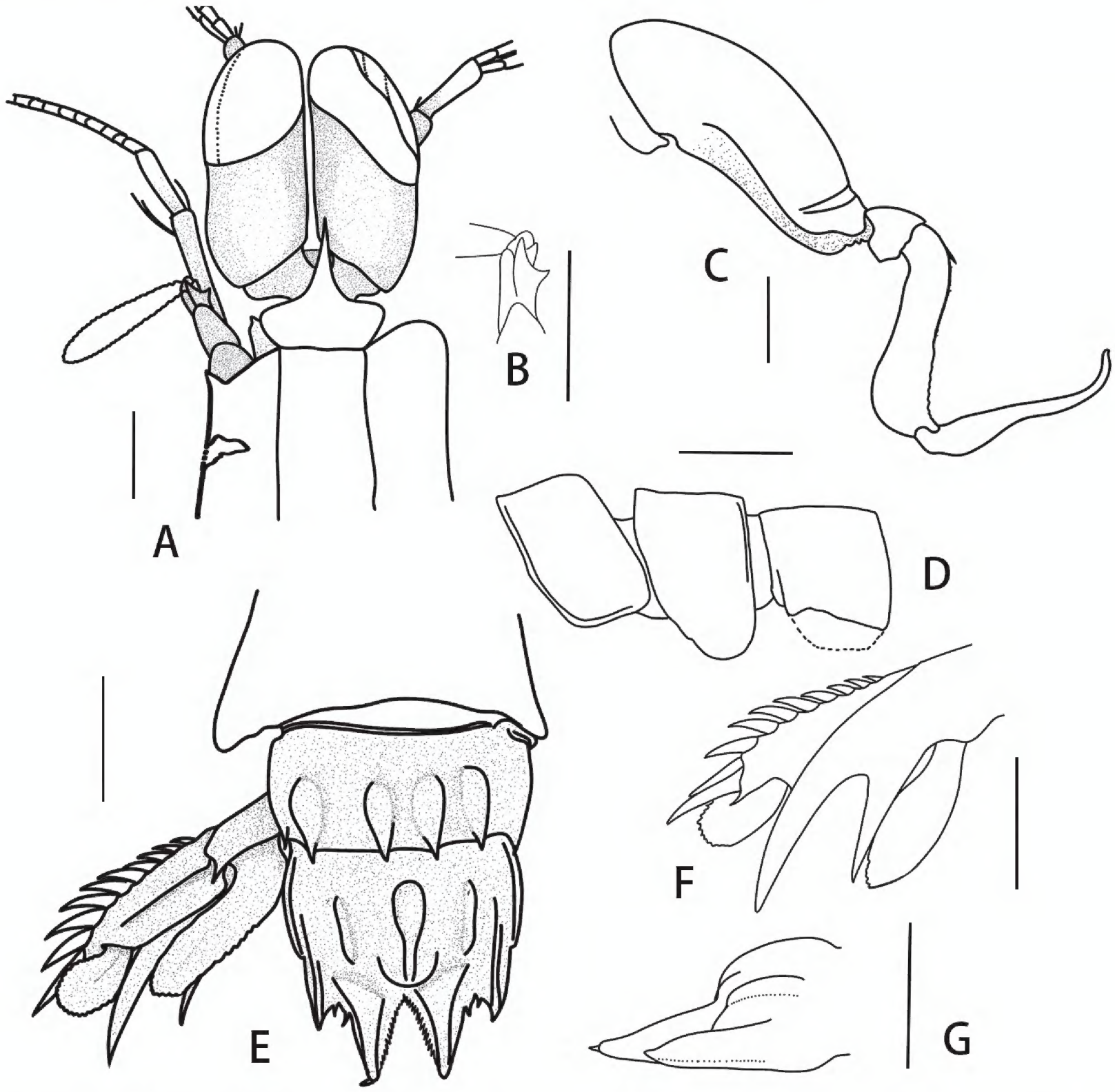

Figure 4. *Gonodactylellus* sp. (MBM288170). Morphological details. **A.** Anterior cephalon, dorsal view; **B.** A2 protopod, left lateral; **C.** Raptorial claw, right lateral view; **D.** TS3–5, right lateral view; **E.** AS5–6, telson and uropod, dorsal view; **F.** Uropod, right ventral view; **G.** Telson, right lateral view. Scale bars: 1 mm (**A–G**).

PLP1 endopod without lateral lobe on posterior endite.

AS1–5 posterolateral angles unarmed. AS6 with armed submedian, intermediate, and lateral bosses.

Telson longer than broad; intermediate teeth distinct, apices extending posteriorly beyond apices of intermediate denticles; lateral teeth distinct, apex blunt, distinct well-off margin of telson. Telson median carina tumid, accessory median carinae short, smooth, fused with median carina posteriorly, not more than half of median carina, anterior submedian carina, submedian expansion longer than half of median carina. Telson ventral surface lacking intermediate teeth or carina on submedian.

Uropodal protopod lateral terminal spines longer; upper proximal surface with blunt spine posteriorly. Uropodal exopod proximal segment outer margin with 10 movable spines, distalmost not exceeding apex of distal segment; inner margin setose; distal margin without ventral spine; exopod distal segment without margin setose. Uropodal endopod narrow, length 2.5, breadth, inner margin setose.

Remarks. This specimen is listed under *Gonodactylellus* Manning, 1995 based on the subcylindrical eyes with the cornea not broader than the stalk, the rostral plate with a slender median spine, and the propodus of the raptorial claw bearing a proximal movable spine (Manning 1995).

Nevertheless, it exhibits a combination of characters not seen in any described species, including a short accessory median carina of the telson fused posteriorly with the median carina, extending not more than half the length of the median carina, and an anterior submedian carina with a submedian expansion longer than half the median carina (Manning 1995; Ahyong 2001, 2012b). Although the general telson shape is somewhat reminiscent of *G. affinis*, it differs in that the median and anterior submedian carinae lack acute posterior spines in this specimen (Manning 1995; Ahyong 2001). Furthermore, it can be separated from *G. caldwelli* by the uropodal protopod which lacks a deeply incised median notch between the paired terminal spines. Due to the absence of key diagnostic structures such as the complete carapace and thoracic somites, it is conservatively identified here as *Gonodactylellus* sp., pending the discovery of additional material.

Gonodactylellus caldwelli Erdmann & Manning, 1998

Fig. 5

Gonodactylellus caldwelli Erdmann & Manning, 1998: 618–619, fig. 1c (type locality: Bira, Spermonde, Indonesia); Debelius, 1999: 273; Ahyong, 2001: 49–51.

Material examined. South China Sea • 4 males, TL 18–20 mm; North Island, Xisha Islands; 16°57'N, 112°18'E; depth 32–44 m; 29 Aug. 2024; Dong Dong coll.; MBM288166 • 4 males, 3 females, TL 20–23 mm; Discovery Reef, Xisha Islands; 16°10'N, 111°42'E; depth 31–40 m; 25 Aug. 2024; Dong Dong coll.; MBM288176 • 1 male, TL 22 mm; South Island, Xisha Islands; 16°56'N, 112°19'E; depth 52 m; 27 Aug. 2024; Dong Dong coll.; MBM288190 • 1 male, TL 24 mm; Shiyu Reef, Xisha Islands; 16°31'N, 111°34'E; depth 58 m; 7 Jul. 2024; Dong Dong coll.; MBM288195 • 1 male, 1 female, TL 23–25 mm; Yinyu Reef, Xisha Islands; 16°34'N, 111°42'E; depth 15–40 m; 20 Aug. 2024; Dong Dong coll.; MBM288206 • 3 females, 1 male, TL 26–28 mm; Vuladdore Reef, Xisha Islands; 16°20'N, 112°2'E; depth 40 m; 26 Aug. 2024; Dong Dong coll.; MBM288208 • 1 female, TL 30 mm; Vuladdore Reef, Xisha Islands; 16°20'N, 112°2'E; depth 40 m; 26 Aug. 2024; Dong Dong coll.; MBM288212 • 4 males, TL 28–32 mm; Zhaoshu Dao, Xisha Islands; 16°59'N, 112°16'E; depth 34–55 m; 30 Aug. 2024; Dong Dong coll.; MBM288214 • 1 male, TL 28 mm; Zhaoshu Dao, Xisha Islands; 16°59'N, 112°16'E; depth 55 m; 31 Aug. 2024; Dong Dong coll.; MBM288184 • 1 male, TL 29 mm; Antelope Reef, Xisha Islands; 16°28'N, 111°33'E; depth 30 m; 22 Aug. 2024; Dong Dong coll.; MBM288215.

Description. Ocular scales are rounded and separate; the rostral plate is elongate, with its length exceeding its width; the anterior margin of the basal portion is transverse, anterolateral angles rounded, and lateral margins slightly divergent anteriorly; the median spine is slender and distinctly longer than the base. The mandibular palp comprises three segments. PLP1 endopod in adult males with lateral lobe on posterior endite. AS5 possesses a sharp, well-developed posterolateral spine. The telson is characterized by prominent IM teeth, apices extending apices of IM denticles; 11–14 SM denticles, while the dorsal surface lacks dense spinules. The accessory MD carinae extend anteriorly to approximately the mid-length of the MD carina, unarmed posteriorly. The anterior SM carinae are unarmed but occasionally exhibit a weakly angular posterior margin. The uropodal exopod proximal segment with 11 movable spines and distal, ventral spine; inner margin of proximal segment and entire margin of distal segment setose. The uropodal endopod is slender, with a length approximately 3.5–4.2 times the width, and bears a single row of setae along its entire margin.

Remarks. The present specimens are consistent with the original description of *Gonodactylellus caldwelli* (Erdmann and Manning 1998). Key diagnostic characters observed include the accessory median carina on the telson extending anteriorly almost to the midlength of the median carina and being unarmed posteriorly, the absence of dorsal spines or spinules on telson carina, and the uropodal exopod possessing a fixed distal spine ventrally on its proximal segment. No significant morphological discrepancies were noted between our specimens and the established descriptions for *G. caldwelli* (Manning 1998).

This finding represents the first formal record of *G. caldwelli* from the South China Sea, extending its known range westward within the tropical western Pacific. Prior to this, *G. caldwelli* was documented to

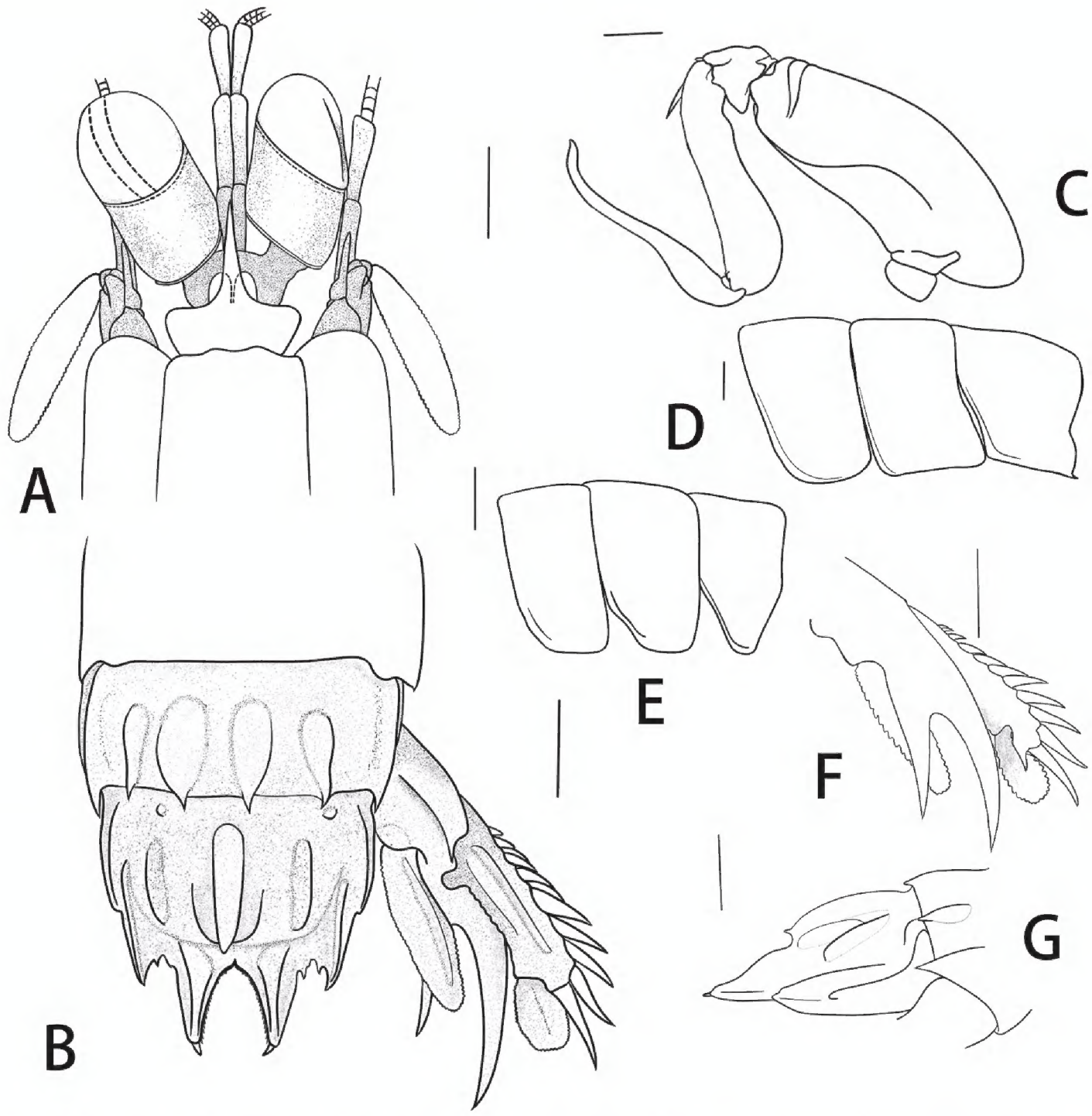

Figure 5. *Gonodactylellus caldwelli* (MBM288212). Morphological details. **A.** Anterior cephalon, dorsal view; **B.** AS5–6, telson and uropod, dorsal view; **C.** Raptorial claw, left lateral view; **D.** AS3–5, right lateral view (MBM288184); **E.** TS6–8, right lateral view; **F.** Uropod, left ventral view; **G.** Telson, right lateral view. Scale bars: 1 mm (**A–G**).

occur from Indonesia (Spermine Archipelago) to northern Australia (Queensland) and Western Australia (Exmouth Gulf) (Ahyong 2001).

Distribution. Indonesia and Australia, from Queensland and Exmouth Gulf, and now the South China Sea.

Discussion

Manning (1995) subdivided the genus *Gonodactylus* sensu lato into five genera: *Gonodactylaceus*, *Gonodactylellus*, *Gonodactylinus*, *Gonodactylus* sensu stricto, and *Neogonodactylus*, while explicitly acknowledging that this classification "lacks phylogenetic support". To date, four of these genera (*Gonodactylaceus*, *Gonodactylellus*, *Gonodactylus*, and *Neogonodactylus*) are still recognized. However, the monophyletic status of the *Gonodactylellus* has remained controversial (Barber and Erdmann 2000; Barber and Boyce 2006), and phylogenetic relationships among *Gonodactylellus* and the other three related genera have yet to be clearly resolved (Ahyong and Jarman 2009; van der Wal et al. 2017; Koga and Rouse 2021). Consistent with previous studies (van der Wal et al. 2017; Koga and Rouse 2021), our phylogenetic results provide strong evidence for a close evolutionary relationship between *Gonodactylellus* and *Gonodactylus*. Phylogenetic analyses based on mitochondrial COI with broad taxon sampling revealed intermixed clades of studied *Gonodactylellus* and *Gonodactylus* species, suggesting non-monophyly in both genera. In contrast, phylogenetic reconstructions using a reduced but information-rich multi-gene dataset revealed the paraphyly of *Gonodactylellus*, while recovering *Gonodactylus* as nested within *Gonodactylellus* under the current sampling. However, the monophyletic status of *Gonodactylus* requires further testing with broader mitogenomic sampling. Despite differences in taxon coverage and gene marker composition, our phylogenetic analyses consistently rejected the monophyly of *Gonodactylellus*, corroborating earlier molecular phylogenetic evidence (Barber and Erdmann 2000; Barber and Boyce 2006; van Der Wal et al. 2017). The persistent non-monophyly of *Gonodactylellus* indicates that the current taxonomic framework does not reflect evolutionary history and may require revision (Ahyong 2001, 2022; Ahyong and Erdmann 2007). Alternatively, this pattern could reflect a complex evolutionary history, potentially involving incomplete lineage sorting, historical hybridization, or morphological convergence. Although our multi-gene framework provides an overall

phylogenetic context for Gonodactylidae, several deeper intergeneric relationships, particularly those involving *Neogonodactylus* and *Gonodactylaceus*, remain weakly supported in the ML analysis. Inclusion of more genomic data (e.g., ultraconserved elements or transcriptomes), extensive taxonomic sampling integrated with detailed morphological examinations, is necessary for future studies to clarify the generic-level phylogenetic relationships and evolutionary history of this group.

In terms of species diversity, our results indicate that the SCS possesses previously underestimated stomatopod diversity, especially within the genus *Gonodactylellus*. Liu (2008) recorded 11 species of stomatopods in Chinese waters, 10 of which are distributed in the SCS, covering three genera: *Gonodactylaceus*, *Gonodactylellus* and *Gonodactylus*. Our study further reveals previously undocumented diversity of stomatopods in the SCS: the first record of *G. caldwelli*, and two undescribed taxa (*G. xishaensis* sp. nov. and *Gonodactylellus* sp.), suggesting that the species richness of stomatopods in the SCS may be underestimated. Notably, the bPTP and ABGD delimitation methods identified 34 and 44 MOTUs, respectively (Fig. 1), exceeding the total number of currently described species of *Gonodactylus* (6 species) and *Gonodactylellus* (25 species). While these methods may overestimate species diversity (Blair and Bryson 2017; Delicado et al. 2025), the observed MOTU patterns reveal substantial genetic heterogeneity within the sampled taxa and may indicate the presence of additional, yet unrecognized lineages. This pattern echoes the findings of Barber et al. (2006): even with a reference database covering 91% of known stomatopod species, the identification results still showed multiple unknown units belonging to families that the database should cover, which were suspected to be undiscovered new species (Barber and Boyce 2006). This further suggests that *Gonodactylus* and its related genera may have higher species richness than currently recognized. Current assessments of stomatopod diversity are still constrained by sampling biases towards dominant species and imperfect specimen preservation. Future work should prioritize comprehensive sampling in understudied areas of the SCS and employ non-invasive sampling techniques (e.g., eDNA metabarcoding) to minimize ecological disturbance (Banerjee et al. 2022).

Conclusion

This study offers new insights into gonodactylid diversity in the SCS by integrating morphological examination with molecular phylogenetic analyses, thereby contributing to a better understanding of regional biodiversity. We document the first occurrence of *G. caldwelli* in the SCS and identify two phylogenetically distinct lineages (*G. xishaensis* sp. nov. and *Gonodactylellus* sp.), indicating that diversity in this region has been underestimated. Our phylogenetic reconstructions corroborate previous studies in recovering *Gonodactylellus* as non-monophyletic, within which *Gonodactylus* was nested under the current sampling. These findings are inconsistent with traditional morphology-based classifications, and suggest that the current taxonomic framework and generic boundaries may not fully reflect true evolutionary relationships. However, due to limited taxonomic coverage, we do not propose formal taxonomic revision at this time. Furthermore, this study underscores the importance of integrative approaches for detecting underestimated diversity in morphologically intricate taxa and refining taxonomic frameworks. Future investigation should enhance sampling efforts, particularly in under-explored regions of the SCS, and integrate additional molecular markers and ecological data to elucidate the mechanisms underlying stomatopod diversification in this region.

Acknowledgements

We would like to express our sincere thanks to Dr. Dong Dong, Dr. Ziming Yuan, and Lin He from IOCAS for their help in sample collection, and to Zhangbo Han for his assistance with the laboratory experiments. We are also grateful to the Editor, Dr. Magdalini Christodoulou, and to the reviewers—including Dr. Shane Ahyong and the anonymous experts—for their constructive and valuable comments on earlier drafts of this manuscript. This work was supported by the Ministry of Science and Technology of China (No. 2021YFF0502801), the National Science & Technology Fundamental Resources Investigation Program of China (No. 2022FY100603), the Technology Fundamental Resources Investigation Program of China (No. 2025FY101400) and the National Natural Science Foundation of China (No. 42276145) and Oceanographic Data Center, IOCAS.

References

Ahyong ST (2001) Revision of the Australian Stomatopod Crustacea. Records of the Australian Museum 26(Supplement 26): 1–326. https://doi.org/10.3853/j.0812-7387.26.2001.1333

Ahyong ST (2002) Stomatopoda (Crustacea) from the Marquesas Islands: results of MUSORSTOM 9. Zoosystema 24(2): 347–372. https://doi.org/10.5281/zenodo.5393319

Ahyong ST (2012a) The marine fauna of New Zealand. Mantis shrimps (Crustacea: Stomatopoda). NIWA Biodiversity Memoir 125: 1–112. [National Institute of Water and Atmospheric Research, NIWA, Wellington, New Zealand]

Ahyong ST (2012b) Stomatopod Crustacea of the KUMEJIMA 2009 Expedition, Japan. Zootaxa 3367(1): 232–251. https://doi.org/10.11646/zootaxa.3367.1.22

Ahyong ST (2016) Results of the comprehensive marine biodiversity survey international workshops 2012 and 2013: Stomatopod Crustacea. The Raffles Bulletin of Zoology (Supplement 34): 455–469.

Ahyong ST (2022) Revision of the Indo-West Pacific coral reef mantis shrimp genus, *Gonodactylopsis* Manning, 1969 (Crustacea: Stomatopoda: Gonodactylidae). Records of the Australian Museum 74(2): 41–57. https://doi.org/10.3853/j.2201-4349.74.2022.1806

Ahyong ST, Erdmann MV (2007) Two new species of *Gonodactylellus* from the Western Pacific (Gonodactylidae: Stomatopoda). The Raffles Bulletin of Zoology 55(1): 89–95. https://doi.org/10.5281/zenodo.4508958

Ahyong ST, Jarman SN (2009) Stomatopod interrelationships: Preliminary results based on analysis of three molecular loci. Arthropod Systematics & Phylogeny 67(1): 91–98. https://doi.org/10.3897/asp.67.e31690

Ahyong ST, Moosa MK (2004) Stomatopod Crustacea from Anambas and Natuna Islands, South China Sea, Indonesia. The Raffles Bulletin of Zoology 11: 61–66.

Banerjee P, Stewart KA, Dey G, Antognazza CM, Sharma RK, Maity JP, Saha S, Doi H, De Vere N, Chan MWY, Lin P-Y, Chao H-C, Chen C-Y (2022) Environmental DNA analysis as an emerging non-destructive method for plant biodiversity monitoring: A review. AoB Plants 14(4): plac031. https://doi.org/10.1093/aobpla/plac031

Barber PH, Boyce SL (2006) Estimating diversity of Indo-Pacific coral reef stomatopods through DNA barcoding of stomatopod larvae. Proceedings Biological Sciences 273(1597): 2053–2061. https://doi.org/10.1098/rspb.2006.3540

Barber PH, Erdmann MV (2000) Molecular systematics of the Gonodactylidae (Stomatopoda) using mitochondrial cytochrome oxidase C (Subunit 1) DNA sequence data. Journal of Crustacean Biology 20(5): 20–36. https://doi.org/10.1163/1937240X-90000004

Barber PH, Erdmann MV, Palumbi SR (2006) Comparative phylogeography of three codistributed stomatopods: Origins and timing of regional lineage diversification in the coral triangle. Evolution; International Journal of Organic Evolution 60(9): 1825–1839. https://doi.org/10.1111/j.0014-3820.2006.tb00526.x

Blair C, Bryson Jr RW (2017) Cryptic diversity and discordance in single-locus species delimitation methods within horned lizards (Phrynosomatidae: Phrynosoma). Molecular Ecology Resources 17(6): 1168–1182. https://doi.org/10.1111/1755-0998.12658

Borradaile LA (1898) On some Crustacea from the Red Sea and Zanzibar. Transactions of the Linnean Society of London, Series 2, 6(3): 389–416.

Capella-Gutiérrez S, Silla-Martínez JM, Gabaldón T (2009) trimAl: A tool for automated alignment trimming in large-scale phylogenetic analyses. Bioinformatics (Oxford, England) 25(15): 1972–1973. https://doi.org/10.1093/bioinformatics/btp348

Cronin TW, Bok MJ, Marshall NJ, Caldwell RL (2014) Filtering and polychromatic vision in mantis shrimps: Themes in visible and ultraviolet vision. Philosophical Transactions of the Royal Society of London, Series B, Biological Sciences 369(1636): 20130032. https://doi.org/10.1098/rstb.2013.0032

Delicado D, Boulaassafer K, Khalloufi N, Hauffe T (2025) A holistic perspective on species delimitation outperforms all methods based on single data types in freshwater gastropods (Caenogastropoda: Hydrobiidae: Pseudamnicola). Zoological Journal of the Linnean Society 203(1): zlae010. https://doi.org/10.1093/zoolinnean/zlae010

Erdmann MV, Manning RB (1998) Preliminary descriptions of nine new stomatopod crustaceans from coral reef habitats in Indonesia and Australia. The Raffles Bulletin of Zoology 46(2): 615–626. https://repository.si.edu/handle/10088/8728

Feller K, Cronin T, Ahyong ST, Porter M (2013) Morphological and molecular description of the late-stage larvae of Alima Leach, 1817 (Crustacea: Stomatopoda) from Lizard Island, Australia. Zootaxa 3722(1): 22–32. https://doi.org/10.11646/zootaxa.3722.1.2

Geller J, Meyer C, Parker M, Hawk H (2013) Redesign of PCR primers for mitochondrial cytochrome c oxidase subunit I for marine invertebrates and application in all-taxa biotic surveys. Molecular Ecology Resources 13(5): 851–861. https://doi.org/10.1111/1755-0998.12138

Kalyaanamoorthy S, Minh BQ, Wong TKF, von Haeseler A, Jermiin LS (2017) ModelFinder: Fast model selection for accurate phylogenetic estimates. Nature Methods 14(6): 587–589. https://doi.org/10.1038/nmeth.4285

Kearse M, Moir R, Wilson A, Stones-Havas S, Cheung M, Sturrock S, Buxton S, Cooper A, Markowitz S, Duran C, Thierer T, Ashton B, Meintjes P, Drummond A (2012) Geneious Basic: An integrated and extendable desktop software platform for the organization and analysis of sequence data. Bioinformatics (Oxford, England) 28(12): 1647–1649. https://doi.org/10.1093/bioinformatics/bts199

Koga C, Rouse GW (2021) Mitogenomics and the phylogeny of mantis shrimps (Crustacea: Stomatopoda). Diversity 13(12): 647. https://doi.org/10.3390/d13120647

Kumar S, Stecher G, Tamura K (2016) MEGA7: Molecular evolutionary genetics analysis Version 7.0 for bigger datasets. Molecular Biology and Evolution 33(7): 1870–1874. https://doi.org/10.1093/molbev/msw054

Liu RY (1975) Preliminary report on the stomatopods (Crustacea) from the Xisha Islands. Studia Marina Sinica 10: 183–197. [in Chinese]

Liu RY (1978) A new genus and two new species of stomatopods (Crustacea) from the South China Sea. Oceanologia et Limnologia Sinica 9(1): 89–93. [in Chinese]

Liu RY (2008) Checklist of Marine Biota of China Seas (Chinese Edition). Science Press, Beijing, 1st edition, 3273 pp.

Liu RY, Wang YL (1998) Two new species of the families Squillidae and Harpiosquillidae (Stomatopoda, Crustacea) from the South China Sea. Oceanologia et Limnologia Sinica 29(6): 588–596. [in Chinese]

Manning RB (1971) Stomatopod Crustacea from the tropical eastern Pacific. Smithsonian Contributions to Zoology 99: 1–58.

Manning RB (1978) Notes on some species of the falcatus group of *Gonodactylus* (Crustacea: Stomatopoda: Gonodactylidae). Smithsonian Contributions to Zoology 258: 1–15. https://doi.org/10.5479/si.00810282.258

Manning RB (1995) Stomatopod Crustacea of Vietnam: The legacy of Raoul Serene. Crustacean Research 4(Special): 1–339. https://doi.org/10.18353/crustacea.Special1995.4_1

Palecanda S, Feller KD, Porter ML (2020) Using larval barcoding to estimate stomatopod species richness at Lizard Island, Australia for conservation monitoring. Scientific Reports 10(1): 10990. https://doi.org/10.1038/s41598-020-67696-x

Patek SN, Caldwell RL (2005) Extreme impact and cavitation forces of a biological hammer: Strike forces of the peacock mantis shrimp *Odontodactylus scyllarus*. The Journal of Experimental Biology 208(19): 3655–3664. https://doi.org/10.1242/jeb.01831

Patek SN, Korff WL, Caldwell RL (2004) Deadly strike mechanism of a mantis shrimp. Nature 428(6985): 819–820. https://doi.org/10.1038/428819a

Rambaut A, Drummond AJ, Xie D, Baele G, Suchard MA (2018) Posterior summarization in Bayesian phylogenetics using Tracer 1.7. Systematic Biology 67(5): 901–904. https://doi.org/10.1093/sysbio/syy032

Ronquist F, Teslenko M, Van Der Mark P, Ayres DL, Darling A, Höhna S, Larget B, Liu L, Suchard MA, Huelsenbeck JP (2012) MrBayes 3.2: Efficient Bayesian phylogenetic inference and model choice

across a large model space. Systematic Biology 61(3): 539–542. https://doi.org/10.1093/sysbio/sys029

Tang RWK, Yau C, Ng W (2010) Identification of stomatopod larvae (Crustacea: Stomatopoda) from Hong Kong waters using DNA barcodes. Molecular Ecology Resources 10(3): 439–448. https://doi.org/10.1111/j.1755-0998.2009.02794.x

Thoen HH, How MJ, Chiou T-H, Marshall J (2014) A different form of color vision in mantis shrimp. Science 343(6169): 411–413. https://doi.org/10.1126/science.1245824

Trifinopoulos J, Nguyen LT, von Haeseler A, Minh BQ (2016) W-IQ-TREE: A fast online phylogenetic tool for maximum likelihood analysis. Nucleic Acids Research 44(W1): W230–W233. https://doi.org/10.1093/nar/gkw256

van der Wal C, Ahyong ST, Ho SYW, Lo N (2017) The evolutionary history of Stomatopoda (Crustacea: Malacostraca) inferred from molecular data. PeerJ 5: e3844. https://doi.org/10.7717/peerj.3844

van der Wal C, Ahyong ST, Adams MWD, Lo N, Ho SYW (2025) Total-evidence phylogenetic analysis resolves the evolutionary timescale of mantis shrimps (Stomatopoda) and provides insights into their molecular and morphological evolutionary rates. Molecular Phylogenetics and Evolution 207: 108346. https://doi.org/10.1016/j.ympev.2025.108346

Vo ST, Pernetta JC, Paterson CJ (2013) Status and trends in coastal habitats of the South China Sea. Ocean and Coastal Management 85: 153–163. https://doi.org/10.1016/j.ocecoaman.2013.02.018

Xiang Y, Guo X, Xiao H, Liu G, Zhou H, Lin Y, Cao H (2023) PhyloSuite 1.2.3: An updated integrated and scalable desktop platform for streamlined molecular sequence data management and evolutionary phylogenetics analysis. Molecular Ecology Resources 23(2): 597–600.

Yu K (2012) Coral reefs in the South China Sea: Their response to and records on past environmental changes. Science China. Earth Sciences 55(8): 1217–1229. https://doi.org/10.1007/s11430-012-4449-5

Supplementary material 1

Supplementary figure

Authors: Shanshan Zheng, Yanrong Wang, Liwen Zhang, Zhongli Sha, Jiao Cheng

Data type: pdf

Explanation note: *In situ* photographs of intact gonodactylid specimens collected in this study.

Copyright notice: This dataset is made available under the Open Database License (http://opendatacommons.org/licenses/odbl/1.0/). The Open Database License (ODbL) is a license agreement intended to allow users to freely share, modify, and use this Dataset while maintaining this same freedom for others, provided that the original source and author(s) are credited.

Link: https://doi.org/10.3897/zse.102.172564.suppl1

Supplementary material 2

Supplementary information

Authors: Shanshan Zheng, Yanrong Wang, Liwen Zhang, Zhongli Sha, Jiao Cheng

Data type: xlsx

Explanation note: **table S1.** Information for gonodactylid species and mitochondrial COI sequences obtained in this study. **table S2.** The mitochondrial COI data obtained from GenBank for the phylogenetic reconstruction in this study. **table S3.** The mitochondrial genes, 18S rRNA, 28S rRNA, and H3 data used for phylogenetic reconstruction in this study. **table S4.** Pairwise Kimura's 2-parameter distances between studied gonodactylid mantis shrimp species based on the mitochondrial COI sequences. **table S5.** Best-fitting substitution model for multi-gene phylogenetic analyses.

Copyright notice: This dataset is made available under the Open Database License (http://opendatacommons.org/licenses/odbl/1.0/). The Open Database License (ODbL) is a license agreement intended to allow users to freely share, modify, and use this Dataset while maintaining this same freedom for others, provided that the original source and author(s) are credited.

Link: https://doi.org/10.3897/zse.102.172564.suppl2

Supplementary material 3

Bayesian inference phylogeny reconstructed from mitochondrial COI sequences

Authors: Shanshan Zheng, Yanrong Wang, Liwen Zhang, Zhongli Sha, Jiao Cheng

Data type: tif

Explanation note: Symbols denote taxonomic novelties: black stars highlight proposed new species (*Gonodactylellus xishaensis* sp. nov. and *Gonodactylellus* sp.), black circles mark newly recorded species (*Gonodactylellus caldwelli*) in the SCS. Posterior probabilities (Pp) above 0.6 are shown for key nodes.

Copyright notice: This dataset is made available under the Open Database License (http://opendatacommons.org/licenses/odbl/1.0/). The Open Database License (ODbL) is a license agreement intended to allow users to freely share, modify, and use this Dataset while maintaining this same freedom for others, provided that the original source and author(s) are credited.

Link: https://doi.org/10.3897/zse.102.172564.suppl3